Volume rendering the neural network in an insect brain in confocal microscopic volume images

Fu-Chi A. Ku and Yu-Tai Ching
Department of Computer and Information Science, National Chiao-Tong University, HsinChu, Taiwan, R.O.C
E-mail: alexku@cis.nctu.edu.tw, ytching@cis.nctu.edu.tw

1. ABSTRACT

Confocal microscopy is an important tool in neural science research. Using proper staining technique, the neural network can be visualized in the confocal microscopic images. It is a great help if neural scientists can directly visualize the 3D neural network. Volume render the neuron fibers is not easy since other objects such as neuropils are also polluted in the staining process and the neuron fiber is thin comparing to the background. Preprocessing of the image to enhance the neuron fibers before volume rendering can help to build a better 3D image of the neural network. In this study, we used the Fourier Transform, the Wavelet Transform, and the matched filter techniques to enhance the neural fibers before volume rendering is applied. Experimental results show that such preprocessing steps help to generate a more clear 3D images of the neural network.

Keywords: neuron fibers visualization, confocal microscopic volume image, Wavelet transform, matched filter, volume rendering.

2. INTRODUCTION

The brain has always been a interesting topic to researchers. It consists of millions of neurons and almost each of them has different functions. Studying the insect brains could help neural scientist to understand the human brains. Directly visualization of the neural network helps researcher to understand the possible interaction between neurons. In this study, we developed preprocessing methods to enhance the neuron fibers to help to get clear 3D images.

Confocal microscopy is a scanning laser technique that allows the recording of 3-D images of small objects usually stained with a fluorescent dye. During the scanning, each voxel is illuminated in turn by a focused laser beam. The photons emitted by the fluorescent dye are filtered by a small pinhole and the remaining photons are detected by a photomultiplier. There are several advantages of confocal microscopy. 1) It is a 3-D detector, by moving the laser header and modifying the intensity of laser beam, the inside voxel can also be illuminated. Therefore, the tissue deformations due to cutting can be avoided. 2) Signal-to-noise ratio is improved. 3) Blurring is reduced. 4) Axial resolution is considerably higher.

Although confocal microscope produces satisfied image than conventional ones, there are still works yet to be done in order to clearly visualize the 3D neural network. First of all, backgrounds still exist, and sometimes overlapped with our target objects. The second is the large variations in image contrast. This made it difficult on automatic thresholding. Third, the object size and intensity across different slices are usually different due to the anatomy position, and the neuron fiber stretches to a variety of directions. So the tracing on target object became a hard work. Due to the problems stated above, it is difficult to have an automatic method to preprocess the images. In this study, we introduce a semi-automatic method to handle the problems above. The presented method employs Fourier Transform, Wavelet Transform and the matched filter techniques.

Wavelet Transform [1][2] and Fourier Transform are widely used on noise reduction. Anca Dima et al. used a 3-D Wavelet Transform on confocal microscopy image [3]. Lin et al. also used it on the segmentation of coronary arteries [4] with matched filter. Khalid A. Al-Kofahi et al. used the neuron topology to extract the tree dimensional structure of a neuron cell [5]. In the conventional methods, a high (or low) pass filter is usually employed to filtrate out undesired signals. In this study, a different way of band information process is applied on the image, that different result is produced. Matched filter is also useful in medical image, especially on vessel detections [6][7]. In

the former study, matched filter is applied to the segmentation of retinal vessels. Like vessel, neuron fibers are also tubular objects so that we use matched filter in our experiments to enhance the fiber.

The data studied is a set of brain images of cockroach. There are 38 slices of images. Each one has resolution 1024×1024. There are two channels in the data set. These two channels present different sets of neural network but have similar backgrounds.

In Section 2, the processing methods are introduced. Experiments and results will be put in Section 3. Finally, conclusion and summaries will be found in Section 4.

3. METHODS

3.1 WAVELET TRANSFORM

A standard Discrete Wavelet Transform (DWT) is summarized as follows and the details can be found in [8][9][10]. The DWT employs a pair of orthogonal high-pass and a low-pass filter to decompose an input signal into high frequency and low frequency components in different resolutions according to the number of levels employed as shown in Figure 1. In the one-dimensional (1-D) case, a signal $x(n)$ is decomposed iteratively by applying the low-pass and the high-pass filters as shown in Figure 1(a). Also a decomposed signal can be reconstruct from its DWT coefficients as shown in Figure 1(b).

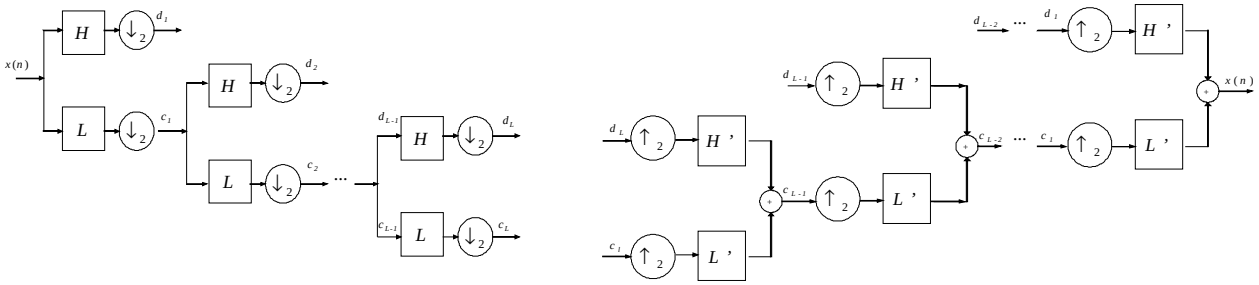

(a) (b)

Figure 1: Multi-level Wavelet (a) decomposition and (b) reconstruction for 1-D case

A two dimensional discrete Wavelet transform (2-D DWT) and its inverse are extended from the one-dimensional transform. It is implemented by applying one-dimensional DWT and IDWT along each of x and y coordinates. In other words, we apply a low-pass filter and a high-pass filter along each of the two coordinates. The original 2-D signal in the form of an image is then divided into four regions:

LL: obtained by applying two low-pass filters on both coordinates,

HL and *LH*: obtained by applying a high-pass filter on one coordinate and a low-pass filter on the other coordinate, and

HH: obtained by applying two high-pass filters on both coordinates.

The 2-D DWT, like the 1-D DWT, can be decomposed iteratively by using the pair of low-pass and the high-pass filters to establish a *k*-stage discrete Wavelet transform on the *LL* component

The first stage of the transform is to decompose the image into four equal size sub-images corresponding to the upper left (LL_1), the upper right (HL_1), the lower left (LH_1), and the low right (HH_1) regions. In the second stage, LL_1 is decomposed into four sub-images again. For the subsequent stage j, the upper left image (LL_{j-1}) is further decomposed to four sub-images. The typical example is illustrated in Figure 2.

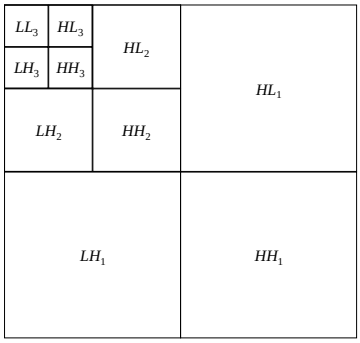

Figure 2: A 2-D 3-stage discrete Wavelet transformation

In the proposed method, we applied the Wavelet transform. Since the edge signals are in high frequency channels, we enhance the *HH*, *HL* and *LH* sub-image on each level. We then reconstruct the original image by using these enhanced sub-images (called *HH'*, *HL'* and *LH'*). The enhancement is shown in equation 1,2 and 3:

$$W(LL_i,\ LH_i,\ HL_i,\ HH_i) = DWT(LL_{i-1}) \quad for\ i \geqq 0,\ \text{where}\ LL_0 = f\ (x,y), \tag{1}$$

$$HH'_i = k \times HH_i \times k,\ HL'_i = k \times HL_i,\ LH'_i = k \times LH_i \qquad \text{where}\ k \in R, \tag{2}$$

$$LL'_{i-1} = IDWT(LL'_i,\ LH'_i,\ HL'_i,\ HH'_i)\ for\ i \geqq 0,\ \text{where}\ LL_0 = f'(x,y). \tag{3}$$

In the equations above, $f(x,y)$ and $f'(x,y)$ denote the original image and the result image. And i denotes the level of discrete Wavelet transform.

The second method needs two channels. Since there are two channels and these two channels have similar background, the second method based on the Wavelet transform takes advantage of this property to reduce the background. An averaged *LL* sub-image is produced simply by taking the average of the *LL* sub-image of the two channels of the same slice as shown in equations (4)-(7).

$$W_a(LL_{ai},\ LH_{ai},\ HL_{ai},\ HH_{ai}) = DWT(LL_{ai-1}) \quad for\ i \geqq 0,\ \text{where}\ LL_{a0} = f_a\ (x,y)$$

$$W_b(LL_{bi},\ LH_{bi},\ HL_{bi},\ HH_{bi}) = DWT(LL_{bi-1}) \quad for\ i \geqq 0,\ \text{where}\ LL_{b0} = f_b\ (x,y) \tag{4}$$

$$LL'_{ai} = LL'_{bi} = (LL_{ai} + LL_{bi}) / 2 \tag{5}$$

$$HH'_{ai} = k \times HH_{ai} \times k,\ HL'_{ai} = k \times HL_{ai},\ LH'_{ai} = k \times LH_{ai} \qquad \text{where}\ k \in R$$

$$HH'_{bi} = k \times HH_{bi} \times k,\ HL'_{bi} = k \times HL_{bi},\ LH'_{bi} = k \times LH_{bi} \qquad \text{where}\ k \in R \tag{6}$$

$$LL'_{ai-1} = IDWT(LL'_{ai},\ LH'_{ai},\ HL'_{ai},\ HH'_{ai})\ for\ i \geqq 0,\ \text{where}\ LL_{a0} = f'_a(x,y)$$

$$LL'_{bi-1} = IDWT(LL'_{bi},\ LH'_{bi},\ HL'_{bi},\ HH'_{bi})\ for\ i \geqq 0,\ \text{where}\ LL_{b0} = f'_b(x,y) \tag{7}$$

In the equations above, $f_a(x,y)$ and $f_b(x,y)$ denote the original image of channel *a* and channel *b*, $f'_a(x,y)$ and $f'_b(x,y)$ denote the resulted image of channel *a* and channel *b*, LL_a, LH_a, HL_a, HH_a, LL_b, LH_b, HL_b and *HHb* denote the *LL*, *LH*, *HL* and *HH* sub-image of channel *a* and channel *b* respectively. And i denotes the level of discrete Wavelet transform.

3.2 MATCHED FILTER

As mentioned previously, the neuron fibers are tubular objects, thus a rectangular matched filter is feasible for enhancing our image. Since matched filter is sensitive to noise, preprocessing of the image is necessary. In our

method, the Fourier Transform and the Wavelet Transform are employed to reduce the background and noise. Afterwards, the Gaussian distribution is introduced to generate this matched filter as shown in Equation (8).

$$g_1(x, y) = 1 - e^{-x^2/2\sigma^2} \tag{8}$$

The proposed matched filter is equipped with two parameters, the orientation θ and the size σ. An angular resolution of 15° was used in the implementation. Due to the various sizes of neuron fibers on thickness, different sizes of matched filters are necessary. In this study, the σ is set from 1 to 3, with a 0.5 increasing in each step. That is, 6 different sizes of matched filter is employed each angel. Each result will be convolved and the strongest response is retained.

4. EXPERIMENTAL RESULTS

4.1 RESULTS OF WAVELET TRANSFORM

In this section, the results produced by the proposed methods are presented. The data set being processed is a confocal microscopic volume image of cockroach brain with 38 slices of a resolution of 1024×1024. Each slice has two channels that come from different kind of dye. Figure 3 and Figure 4 shows the original image and the volume rendered results respectively. Since the between-pixel-distance on *x*, *y* and *z* axis are distinct (*x* : *y* : *z* = 1.12 : 1.12 : 4), so the resizing of the image is necessary. The new size of the image is 287×287×38. Volpack 1.0-b3, which is designed by Stanford University is employed as the volume rendering tool.

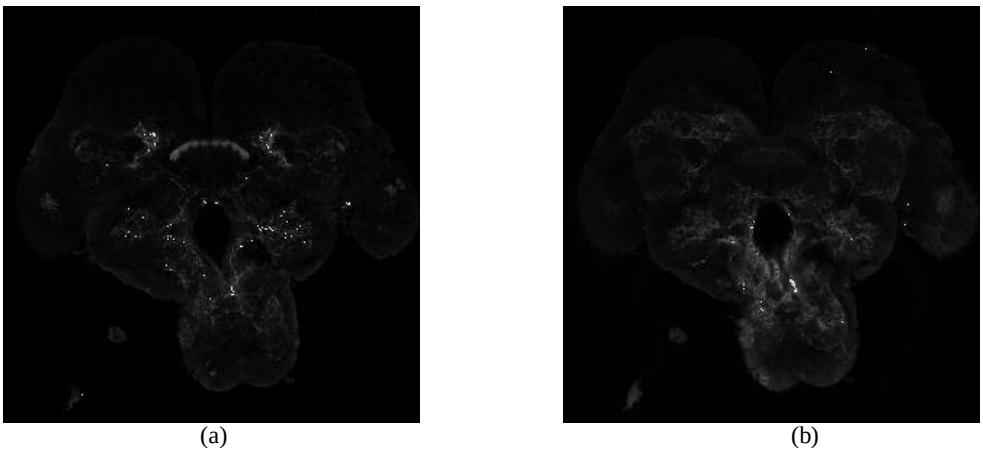

(a) (b)

Figure 3: slice 19 of the dataset (a) is the first channel (b) is the second channel

Observe that, the two channels have similar background. The second method of Wavelet transform can be applied. Figure 4 shows the volume rendering results obtained from the original, unprocessed image. The unwanted objects mixed with the desired neuron fibers after volume rendering. In Figure 5, the result of applying the first method of Wavelet transform is presented, and the second method of Wavelet transform is shown in Figure 6.

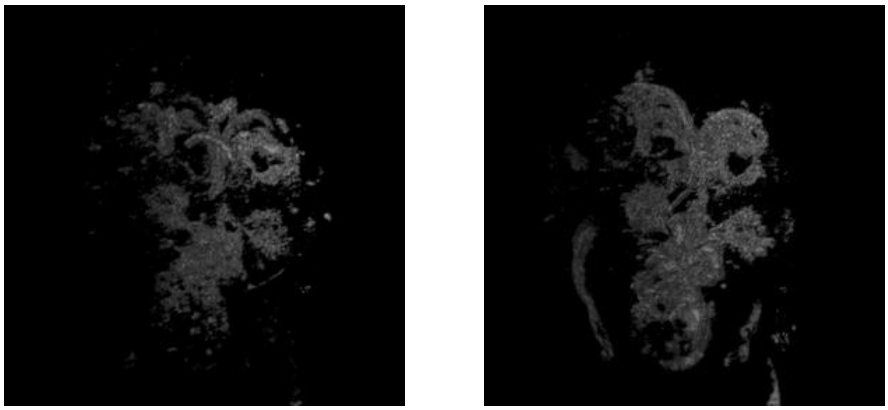

(a) (b)

Figure 4: the volume rendered image of the unprocessed image from (a) the first channel and (b) the second channel

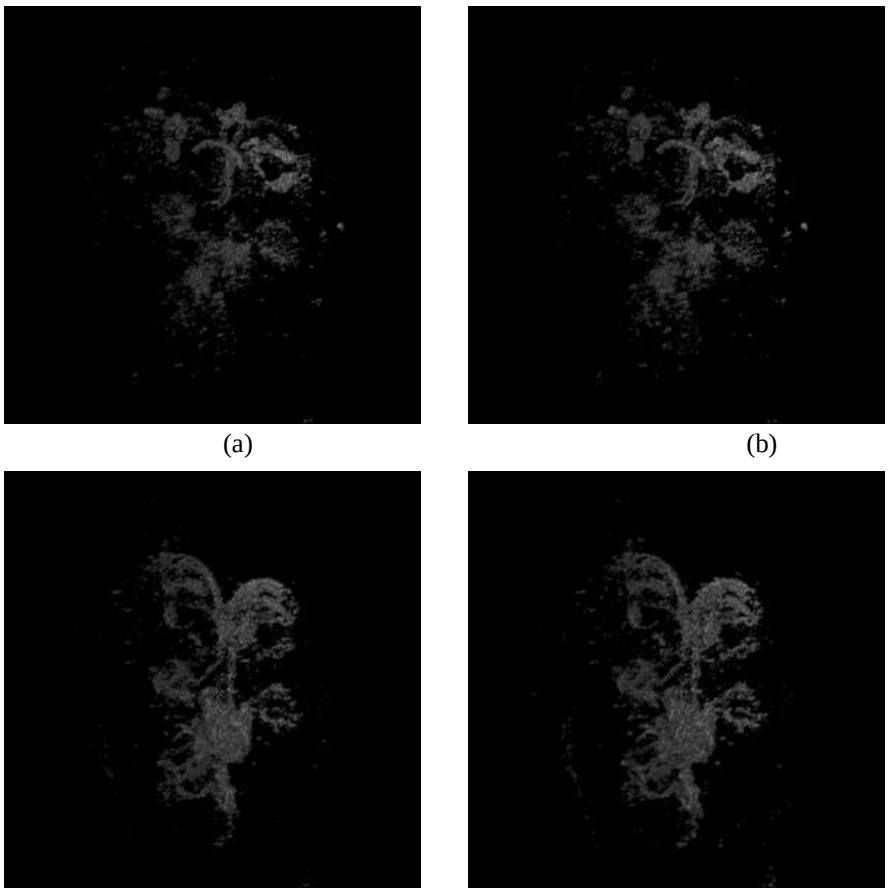

(a) (b)

(c) (d)

Figure 5: the volume rendering result after applying the first method of Wavelet transform. (a) a 3-level (b) a 4-level Wavelet transform for the first channel (c) a 3-level (d) a 4-level Wavelet transform for the second channel

Comparing Figure 4 and 5, it can be found that the fiber is indeed enhanced, backgrounds have been eliminated, but unwanted objects which cover neuron fiber still remained.

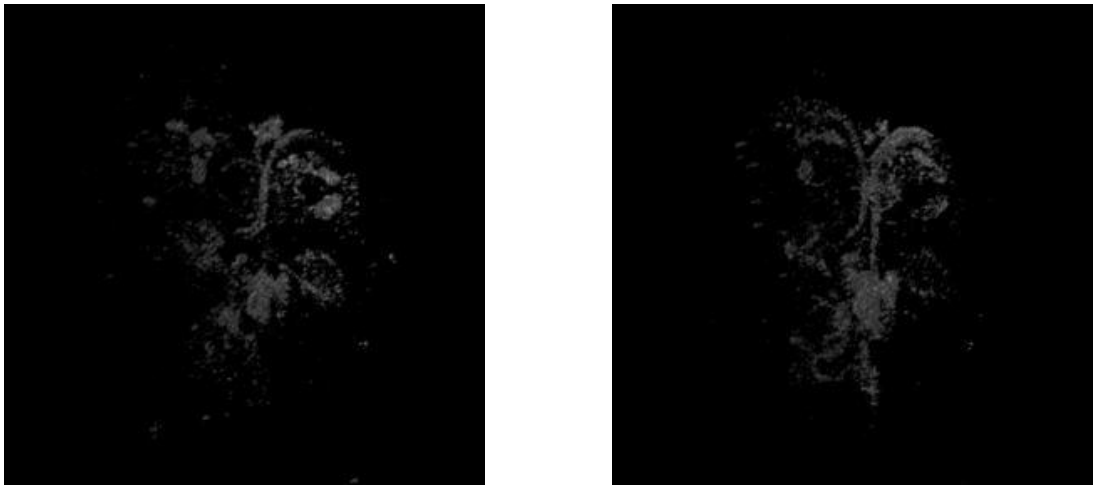

(a) (b)

Figure 6: the results after applying the second method of Wavelet transform (a) channel 1 and (b) channel 2

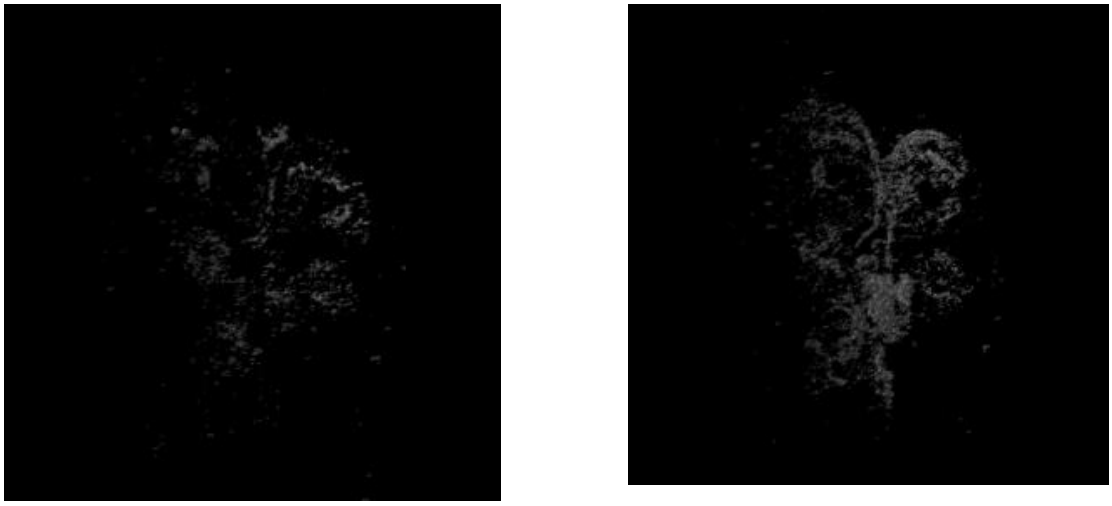

(a) (b)

Figure 7: The result obtained by applying Fourier Transform (a) the first channel, (b) the second channel

As shown in Figure 7, Fourier Transform is able to remove the background, but some of the desired objects are removed as well. The second method of Wavelet transform is better than the former one and Fourier transform.

4.2 RESULTS OBTAINED BY USING THE MATCHED FILTER

In this section, the results after applying the matched filter are presented. Figure 8 shows the result obtained by rendering the volume obtained by applying the matched filter to the original image. Figure 9 shows the result after first applying Fourier transform followed by the matched filter. Figure 10 shows the image obtained by applying a 3-level Wavelet transform followed by matched filter.

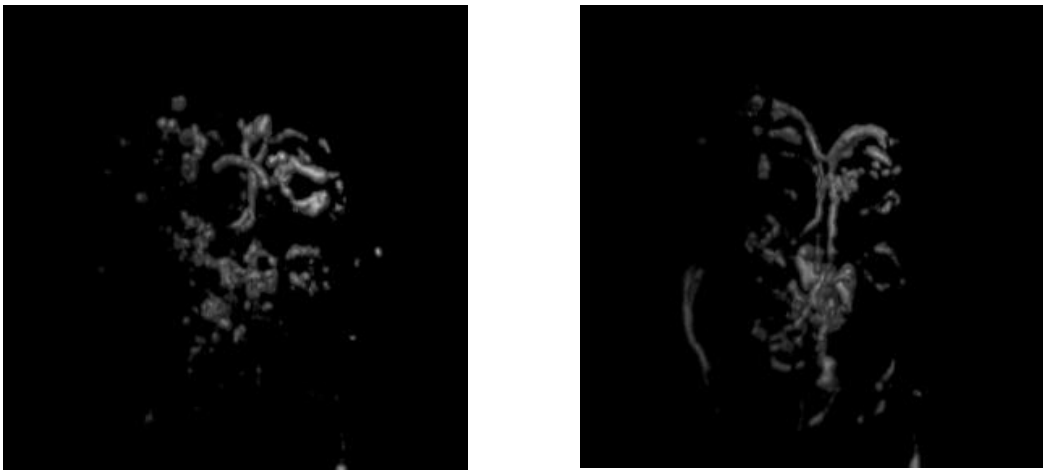

(a) (b)

Figure 8: results obtained by applying the matched filter to the original image (a) the first channel (b) the second channel

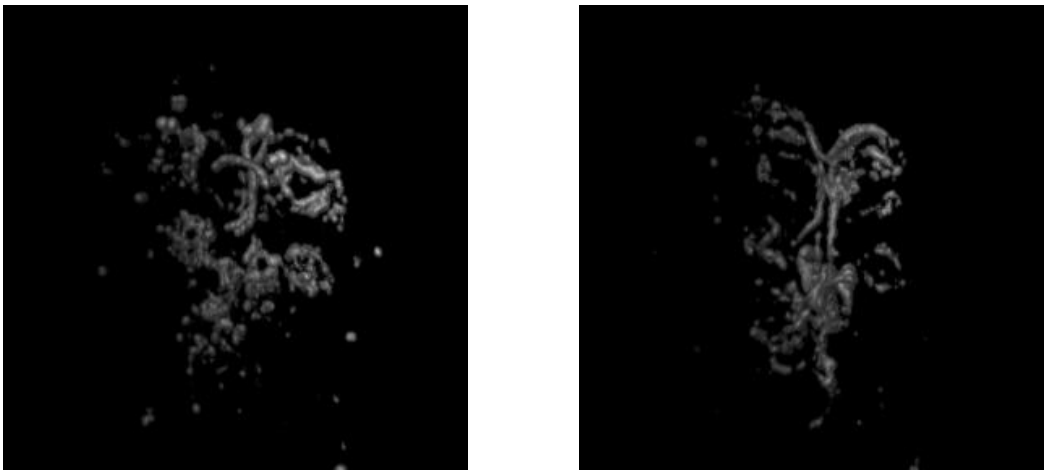

(a) (b)

Figure 9: results obtained by applying Fourier Transform image followed by matched filter (a) the first channel (b) the second channel.

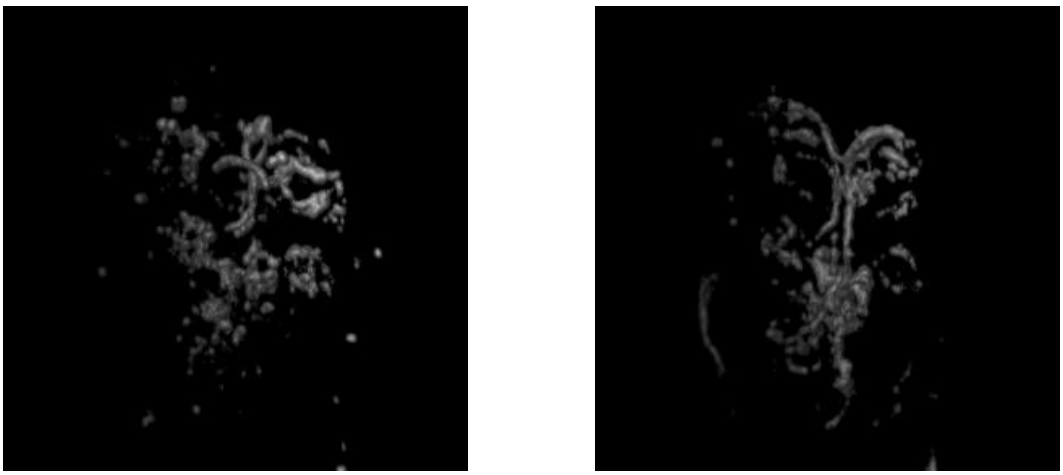

(a) (b)

Figure 10: results obtained by applying a 3-level Wavelet transform followed by the matched filter (a) the first channel (b) the second channel

Although Figure 8 and Figure 9 looks "cleaner" than Figure 10, but the image of Figure 10 is better than Figure 8 and Figure 9 due to the conservation of desired signals.

5. CONCLUSIONS AND SUMMARIES

In this study, we used the Wavelet transform to enhance the neuron fibers in confocal microscopic images. The first method of Wavelet transform is to multiply a constant *k* to *HH*, *HL*, and *LH* sub-images to enhance the high frequency components (the edge information are in the high frequency component). The second is to compute a new *LL* sub-image by subtracting the average of *LL* sub-images of two channels. Since the two channels have similarity backgrounds, this method works well to remove the common background. The second experiment is to apply the matched filter. In this experiment, the Wavelet transform follow by matched filter performed better than the other methods.

6. ACKNOWLEDGEMENTS

We thank to Professor A. S. Chiang, Department of Life Science, National Tsing Hua University, Hsinchu, Taiwan, for providing the data sets. This work was supported in part under the grant NSC-90-2213-E-009-119, National Science Council, Taiwan.

8. REFERENCES

1. Eric J. Stollnitz, Tony D. DeRose, and David H. Salesin, "Wavelets for Computer Graphics. Theory and Applications" Morgan Kaufmann Publishers, Inc., 1996.
2. Unser, Michael,1996."Wavelets, statistics, and biomedical applications," *8th IEEE Signal Processing Workshop on Statistical Signal and Array Processing*, Jun 1996 pp.: 244 -249
3. Anca Dima, Michale Scholz, and Klaus Obermayer, 2002. "Automatic Segmentation and Skeletonization of Neurons From Confocal Microscopy Images Based on the 3-D Wavelet Transform," *IEEE Transactions on Image Processing*, July, Vol. 11, NO. 7, pp. 790-801
4. Chih-Yang Lin, Yu-Tai Ching, S. James Chen, "Extraction of Coronary Arterial Tree Using Cine X-Ray Angiograms"
5. Khalid A. Al-Kofahi, Sharie Lasek, Donald H. Szarowski, Christopher J. Pace, and George Nagy, 2002. "Rapid Automated Three-Dimensional Tracing of Neurons From Confocal Image Stacks," IEEE Transactions on Information Technology in Biomedicine, June, Vol. 6, No. 2, pp. 171-187.
6. Chatterjee, S.; Chaudhuri, S.; Goldbaum, M.; Katz, N.; Nelson, M., 1989,"Detection of blood vessels in retinal images using two-dimensional matched filters," *IEEE Transactions on Medical Imaging*, Volume: 8 Issue: 3 , Sep 1989, pp. 263 -269
7. Goldbaum, M.; Hoover, A.D.; Kouznetsova, V., 2000, "Locating blood vessels in retinal images by piecewise threshold probing of a matched filter response," *IEEE Transactions on Medical Imaging*, Vol.: 19 Issue: 3 , Mar 2000, pp. 203 -210
8. S. Mallat, "A Theory fro Multiresolution Signal Decomposition: The Wavelet Representation," IEEE Trans.PAMI, vol. 11, pp. 647-693, 1999.
9. P. P. Vaidyanathan, "Multirate Systems And Filter Banks", Prentice Hall, Inc., 1993.
10. L. Cohen, "Time-Frequency Distributions - A Review," Proc. IEEE, Vol. 77, pp. 941-981, 1989